ChemPubSoc Europe

DOI: 10.1002/chem.201904526

CHEMISTRY A European Journal Full Paper

Phosphors

A Double-Band Emitter with Ultranarrow-Band Blue and Narrow-Band Green Luminescence

Freia Ruegenberg,[a] Markus Seibald,[b] Dominik Baumann,[b] Simon Peschke,[b] Philipp C. Schmid,[b] and Hubert Huppertz*[a]

Abstract: Understanding the origin and mechanisms of luminescence is a crucial point when it comes to the development of new phosphors with targeted luminescence properties. Herein, a new phosphor belonging to the substance class of alkali metal lithosilicates with the generalized sum formula $Cs_{4-x-y-z}Rb_xNa_yLi_z[Li_3SiO_4]_4:Eu^{2+}$ is reported. Single crystals of the cyan-emitting UCr_4C_4-type phosphor show a peculiar double-band luminescence with one ultranarrow emission band at 473 nm and a narrow emission band at 531 nm under excitation with UV light ($\lambda_{exc} = 408$ nm). Regarding occupation of the channels by the light metal ions, investigations of single-crystal XRD data led to the assumption that domain formation with distinct lithium- and sodium-filled channels occurs. Depending on which of these channels hosts the activator ion Eu^{2+}, a green or blue emission results. The herein-presented results shed new light on the luminescence process in the well-studied UCr_4C_4-type alkali metal lithosilicate phosphors.

Introduction

In recent years, the search for alternative light sources and the ongoing development of light-emitting diodes (LEDs) to produce white light has led to a series of discoveries in the field of phosphor materials. One of the most promising approaches to more economical white-light illuminants is the phosphor-converted LED (pc-LED).[1] In this concept, a UV or blue primary LED is combined with one or more phosphors that convert part of the short-wavelength primary light to longer wavelengths in the visible spectrum in order to achieve the desired overall white emission. Nowadays, common substance classes for inorganic phosphors for application in pc-LEDs are, for example, garnet materials such as $YAG:Ce^{3+}$[2] with yellow emission, rare earth doped oxonitrides such as β-$SiAlON:Eu^{2+}$[3] as the green component, and $CaAlSiN_3:Eu^{2+}$[4] or $(Ba,Sr)_2Si_5N_8:Eu^{2+}$ phosphors[5] as the red component.

In addition to the orthosilicate phosphors $Sr_3SiO_5:Eu^{2+}$[6] and Ba^{2+}-co-doped $Sr_3SiO_5:Eu^{2+}$,[7] latterly, the class of alkali metal lithosilicates entered the stage of promising phosphor materials. Firstly described by Hoppe et al. in 1994,[8] alkali metal lithosilicates have been rediscovered as suitable host materials for activator ions such as Eu^{2+} and have put forth a few representatives with remarkable luminescent properties. Dutzler et al. published $Na[Li_3SiO_4]$, $K[Li_3SiO_4]$, and $NaK_7[Li_3SiO_4]_8$ with ultranarrow blue, broadband, and yellow-green double-band emission, respectively, when doped with Eu^{2+}.[9] Independently, Sato et al. reported the same compound $Na[Li_3SiO_4]:Eu^{2+}$ with slightly different emission spectra.[10] Zhao et al. reported furthermore the cyan emitting compound $Na_{0.5}K_{0.5}[Li_3SiO_4]:Eu^{2+}$[11] and green-emitting $RbLi[Li_3SiO_4]_2:Eu^{2+}$.[12] Recently, Liao et al. detected green luminescence in the sodium analogue of the latter, $RbNa[Li_3SiO_4]_2:Eu^{2+}$.[13]

Additionally, Xia et al. published the phosphors $RbNa_2K[Li_3SiO_4]_4:Eu^{2+}$ (RNKLSO:Eu^{2+}), $CsNa_2K[Li_3SiO_4]_4:Eu^{2+}$ (CNKLSO:Eu^{2+}),[14] and $RbNa_3[Li_3SiO_4]_4:Eu^{2+}$ (RNLSO:Eu^{2+}).[15] Dutzler et al. were the first to add a sodium-free compound, namely $RbKLi_2[Li_3SiO_4]_4:Eu^{2+}$ (RKLSO:Eu^{2+}), to this series of alkali metal lithosilicates.[16] All of the above-mentioned compounds can be described by the general formula $A_4[Li_3SiO_4]_4$, where A stands for the alkali metal cations (Na, K, Rb, and Cs) and the brackets enclose the lithosilicate framework. Alkali metal lithosilicates of this kind regularly crystallize in the space group *I*4/*m* and can thus be easily related to the UCr_4C_4 structure type. Despite the similar sum formula, these compounds must be distinguished from the aforementioned $RbLi[Li_3SiO_4]_2:Eu^{2+}$ and $RbNa[Li_3SiO_4]_2:Eu^{2+}$, which are assigned to space group *C*2/*m* and exhibit different properties due to the different structure.

The basic structure of the UCr_4C_4-type alkali lithosilicates is built up by a network of edge- and corner-sharing $[LiO_4]$ and $[SiO_4]$ tetrahedra. This rigid network forms two different kinds

[a] F. Ruegenberg, Prof. Dr. H. Huppertz
Institute of General, Inorganic and Theoretical Chemistry
University of Innsbruck, Innrain 80–82, 6020 Innsbruck (Austria)
E-mail: hubert.huppertz@uibk.ac.at

[b] Dr. M. Seibald, Dr. D. Baumann, Dr. S. Peschke, Dr. P. C. Schmid
OSRAM Opto Semiconductors GmbH
Mittelstetter Weg 2, 86830 Schwabmünchen (Germany)

Supporting information and the ORCID identification number(s) for the author(s) of this article can be found under: https://doi.org/10.1002/chem.201904526.

of vierer-ring channels[17] along the crystallographic *c* axis. The first vierer-ring channel is made up exclusively of [LiO_4] tetrahedra. Therefore, it forms highly symmetric channels, in which the heavier alkali metal cations are located in eightfold, cube-like coordination by oxygen atoms. The other type of vierer-ring channels consists of [LiO_4] and [SiO_4] tetrahedra and is hence slightly distorted. In the above-described compounds, these channels host the lighter alkali metal cation sodium. In the general formula $A_4[Li_3SiO_4]_4$, *A* represents the alkali metal cations present in the channels and the brackets indicate the composition of the lithosilicate framework. Their common features, namely the ultranarrow-band blue-to-cyan emission in combination with good thermal and chemical stability, make them potential candidates for use in white-light pc-LEDs when combined with another, narrow-band, red-emitting phosphor. Suitable for this purpose would be the red-emitting $Sr[LiAl_3N_4]:Eu^{2+}$ (SLA) by Pust et al.[18] or the brilliant red-emitting $Sr[Li_2Al_2O_2N_2]:Eu^{2+}$ (SALON) by Hoerder et al.[19] Recently, red-emitting oxide-based phosphor $Rb_3YSi_2O_7$:Eu was discovered by Xia et al.[20]

The peculiar ultranarrow-band blue luminescence could be observed in all UCr_4C_4-type alkali metal lithosilicates having sodium-containing channels. The only exception so far is the recently discovered $RbKLi_2[Li_3SiO_4]:Eu^{2+}$, which was published by Dutzler et al.[16] Although there are no sodium-containing channels in the structure, under certain conditions this compound shows blue luminescence at 474 nm when doped with Eu^{2+}.

Herein, we present a new UCr_4C_4-type alkali metal lithosilicate with general sum formula $Cs_{4-x-y-z}Rb_xNa_yLi_z[Li_3SiO_4]_4:Eu^{2+}$, which is hence the first representative with both Na and Li cations in the vierer-ring channels made up by [LiO_4] and [SiO_4] tetrahedra. Single-crystals of the compound, the exact composition of which varies slightly with respect to the alkali metal ions in the vierer-ring channels, show a peculiar double-band luminescence with two defined peaks in the blue and green spectral region under excitation with UV light. This indicates the presence of two distinct emission centers in the structure. Subsequently, we provide structure–property relationships as an explanation for this extraordinary luminescence behavior.

Results and Discussion

Crystal structure

UCr_4C_4-type alkali metal lithosilicates are characterized by a rigid network of [LiO_4] and [SiO_4] tetrahedra, which is relatively insensitive to the insertion of alkali metal ions of various radii into the different vierer-ring channels. This fact above all affects the appearance of the powder XRD (PXRD) patterns in a complicating way. Although the size differences between, for example, the cesium and the rubidium cation are remarkable, the lattice parameters change only slightly if comparing, for instance, $RbNa_2K[Li_3SiO_4]_4$ ($a = 10.9677(2)$, $c = 6.2964(1)$ Å) and $CsNa_2K[Li_3SiO_4]_4$ ($a = 10.9936(3)$, $c = 6.3481(2)$ Å). In consequence, the reflection positions and intensities in the PXRD patterns of the UCr_4C_4-type alkali metal lithosilicates are quite similar, which complicates the distinction of the substances or a statement about the exact composition, such as mixed occupations, by PXRD and Rietveld refinement. For this reason, PXRD was considered to be an unsuitable method for an accurate determination of the crystal structure and composition of $Cs_{4-x-y-z}Rb_xNa_yLi_z[Li_3SiO_4]_4:Eu^{2+}$, so small single-crystals were carefully grown and isolated for a single-crystal structure analysis.

A first structure refinement of one of the single-crystals led to the sum formula $Cs_{0.45(2)}Rb_{0.87(2)}Na_{1.68(1)}Li_1[Li_3SiO_4]_4$, (hereinafter abbreviated as CRNLLSO), whereby the activator ion Eu^{2+} was initially not taken into account. Like most of the UCr_4C_4-type alkali metal lithosilicates, this compound crystallizes in tetragonal space group *I*4/*m*. The lattice parameters are $a = 10.972(2)$ Å and $c = 6.3531(7)$ Å and are therefore in the same range as those of the other representatives. The anisotropic refinement led to final values of $R1 = 3.9\%$ and $wR2 = 10.9\%$ for all data, and the R_{int} value of 5.06% indicates a reliable refinement result.

In the refined structure presented in Figure 1, the highly symmetric vierer-ring channel (in the following denoted CH1) hosts the heavier alkali metal ions. Alternately, there is one mixed site with Cs^+ and Rb^+ and another mixed site with Rb^+ and Na^+ located in an eightfold, cube-like coordination sphere.

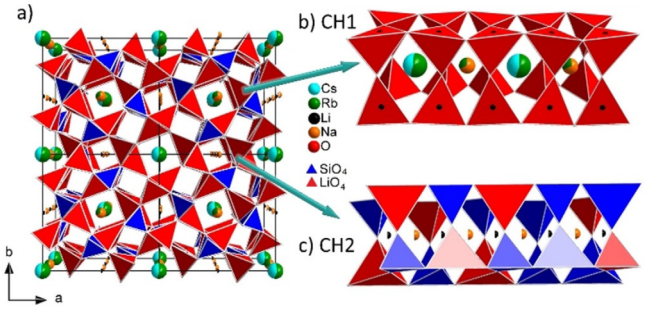

Figure 1. Projection view of the undoped structure of CRNLLSO. a) View of a quadruple cell along [00$\bar{1}$]. b) Detailed side view of channel CH1, which contains the mixed heavy-alkali-metal cation sites Rb/Cs and Rb/Na in an alternating sequence. c) Detailed side view of CH2 containing Na^+ positions (50% occupation) in the distorted cube-like coordination sphere and the Li cations on the approximately square-planar-coordinated site (occupation: 50%).

In the other vierer-ring channel, in the following denoted CH2, the refinement yielded one Na^+ with 50% occupation probability on the distorted eightfold, cube-like coordination position and one Li^+ with 50% occupation probability on the approximately square-planar coordination position in between. Of course, these mixed and half-occupations do not fully correspond to reality in the crystal and arise from the statistical averaging of the occupancies over the whole crystal.

Looking at the Cs^+/Rb^+ position reveals that the obtained bond length to the oxygen anions in the cube-like, eight-fold coordination sphere is 3.050(3) Å. For theoretical Cs–O and Rb–O bond lengths[21] weighted by the Cs^+/Rb^+ ratio on this

site, a calculated value of 3.09 Å was obtained, which is in good accordance with the refined value. Because the framework is very rigid, it can be assumed that this site is already completely used to its maximum capacity by a Cs^+/Rb^+ ratio of about 45:55 and that further introduction of the larger cesium ions is no longer possible, even if an excess is applied (see below). By performing the same routine with the Rb^+/Na^+ site, a calculated value of 2.53 Å was obtained, which is quite a bit smaller than the refined Rb^+/Na^+–O bond length of 2.805(3) Å. This deviation may also arise from the stiffness of the rigid framework and suggests that larger ions could still be introduced at this position in CH1. This applies as well to the activator ion Eu^{2+}, which would fit well in an eightfold oxygen coordination with a theoretical Eu–O bond length of 2.67 Å. However, other arguments speak against this position in CH1 as a doping site: to ensure charge balance, the activator ion Eu^{2+} should displace two singly charged cations when introduced into the structure. Clearly, these would be the neighboring ions, which in the case of CH1 are Cs^+ or Rb^+. Due to the heaviness of the cations and the good fitting accuracy at this position, a high energy barrier is expected.

However, it is a different matter for light-metal channel CH2. Here, the eightfold-coordinated site is half-occupied by Na^+, with Na–O bond lengths of 2.473(3) and 2.689(4) Å. The theoretically calculated Na–O bond length of 2.60 Å is consistent with the refined values. The same also holds for Li^+ on the almost square-planar site with a theoretical Li–O bond length of 1.97 Å and refined values of 1.895(4) and 2.169(4) Å.

With a theoretical Eu–O bond length of 2.67 Å, Eu^{2+} would therefore fit very well into the center of the cube-like coordinated position. Positioning of Eu^{2+} on the square-planar-coordinated Li^+ position, however, is not considered possible owing to space constraints.[22] Thus, if charge balance and the dimensions of the coordination polyhedral in question are taken into account, it is more likely that the activator ion Eu^{2+} is located in CH2 on the Na^+ position and that it replaces two Na^+ cations, two Li^+ cations, or one Na^+ and one Li^+ cation.

Luminescence

Another indication for the location of the activator site in channel CH2 on the eightfold-coordinated Na^+ site is the similarity of the blue luminescence peak to that of the narrow-band blue emitter $Na[Li_3SiO_4]:Eu^{2+}$[9] (NLSO). NLSO has a peak maximum at 469 nm with a full width at half-maximum (FWHM) of 32 nm, and in the structure, only the Na^+ position can be considered for doping. The site is located in a slightly distorted vierer-ring channel made up of $[LiO_4]$ and $[SiO_4]$ tetrahedra, just like in the new phosphor, and is coordinated by 7 + 1 oxygen ions with Na–O bond lengths varying from 2.419(2) to 2.741(2) Å. Luminescence investigations on a single-crystal of $CRNLLSO:Eu^{2+}$ yielded an ultranarrow blue peak with a calculated maximum at 472.7 nm and an FWHM of 25.2 nm (0.14 eV) as well as a narrow green emission peak at 530.5 nm with an FWHM of 58.0 nm (0.24 eV). The Na^+ site in CH2 of CRNLLSO has a similar environment to the Na^+ cation in NLSO, whereas differences in the position of the peak maximum may result from the diverse second coordination sphere, and the smaller FWHM may be explained by the higher symmetry around the Na^+ site in CRNLLSO.

However, the origin of the green emission band remains to be discussed. Apparently, there must still be a distinguishable second emission center, in which the activator ion is situated on about an equal footing with the blue emission center. This is evident from the thermal quenching behavior of the tested powder sample. As shown in Figure S1 in the Supporting Information, the green and the blue luminescence bands are quenched evenly with increasing temperature, which argues for two symmetrically equivalent emission centers. At typical operating temperatures of 100–150 °C, the thermal quenching behavior is moderate with a drop in relative integral intensity of only 5–14% (see Figure 3). To clarify the location of the green emission center, it is useful to take a closer look at the structure of $CRNLLSO:Eu^{2+}$ and to make comparisons to the original publication on UCr_4C_4-type alkali metal lithosilicates of Hoppe et al. from 1994. Hoppe et al. described, for example, the structure of $CsKNaLi[Li_3SiO_4]_4$, which in addition to the new compounds CRNLLSO and $RKLSO:Eu^{2+}$[16] is the only known UCr_4C_4-type alkali metal lithosilicate in which, according to single-crystal refinement, the vierer-ring channels host Li^+ cations. Hoppe et al. found an Na^+ cation with 50% occupation probability on the eightfold, cube-like coordination position and an Li^+ cation with 50% occupation probability on the approximately square-planar coordination position in CH2, too. Alternating filling with an Na^+ and an Li^+ cation in every second coordination sphere is impossible in terms of space, as the distance from Na^+ to its neighboring Li^+ cations would be 1.60 Å on one side and 4.79 Å on the other. Similar values are obtained with CRNLLSO: in the case of an alternating filling of CH2, the distance of the Na^+ cations to the neighboring Li^+ cations would be 1.59 Å on the one side and 4.76 Å on the other.

However, Hoppe et al. suggested domain formation towards distinct Li^+- or Na^+-containing vierer-ring channels. This domain formation can occur in two ways: The Na^+- and Li^+-containing channels are completely separated from each other, or there is stacking of the domains within the channel. In the latter case, there would have to be a defect when switching between the individual domains, so that either a Li^+ or Na^+ site remains unoccupied. Keeping this in mind, the idea is that different luminescence occurs, depending on whether the activator ion is in an Na^+ or an Li^+ domain. The position of the activator ion remains the same in both cases, that is, the center of the cube-like coordinated site, as shown in Figure 2. Of course, filling of the vierer-ring channel affects its structure, so that an activator ion in an Na^+-containing channel would have a different environment and thus different luminescence properties than one in an Li^+-containing channel. Owing to the structural similarity to NLSO and the blue luminescence in UCr_4C_4-type alkali metal lithosilicates in which CH2 hosts only Na^+ cations, such as $RbNa_2K[Li_3SiO_4]_4:Eu^{2+}$ ($RNKLSO:Eu^{2+}$), $CsNa_2K[Li_3SiO_4]_4:Eu^{2+}$ ($CNKLSO:Eu^{2+}$), and $RbNa_3[Li_3SiO_4]_4:Eu^{2+}$ ($RNLSO:Eu^{2+}$), we suggest that doping Eu^{2+} into such an Na^+ domain causes blue luminescence. At

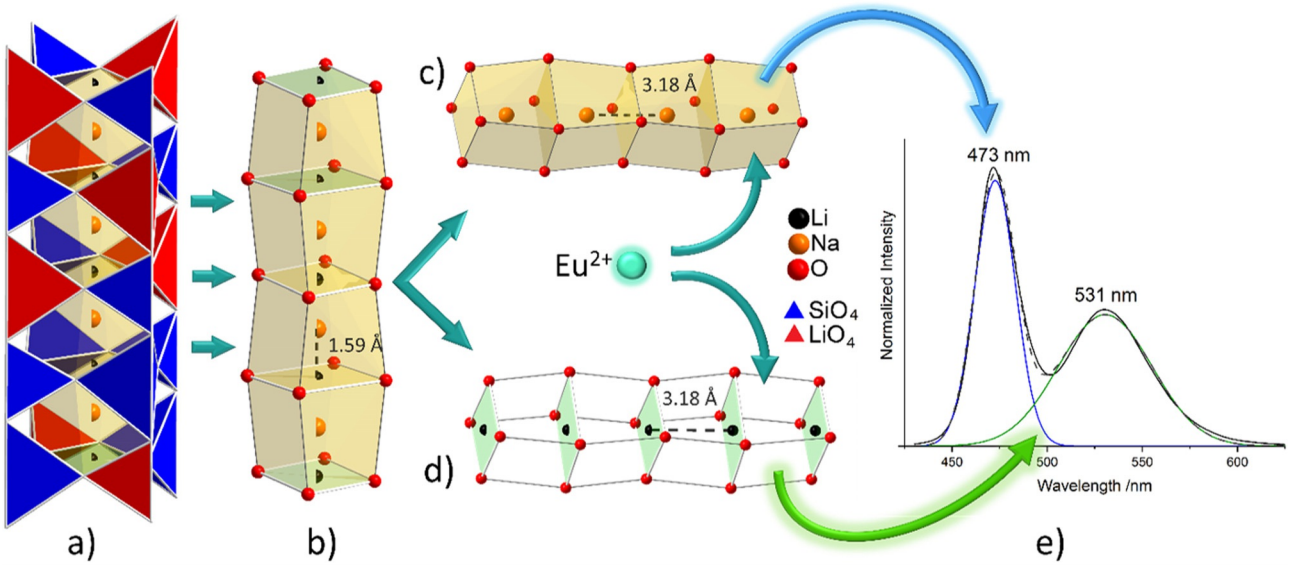

Figure 2. In-depth view and breakdown of the domain formation in CH2. An overall view of channel CH2 is given in a). b) Details of the theoretical filling of CH2 obtained from the refinement, with alternating Li^+ and Na^+ ions (in each case with 50% occupation) and the coordination polyhedra with the oxygen anions. c,d) Breakdown of the data into the two distinct domains that can be formed: In c), solely Na^+ ions occupy the channel on the eightfold, distorted cube-like coordination site. In d), CH2 is populated by the Li^+ ions, which are located in a square-like, nearly planar coordination sphere. If the activator ion Eu^{2+} is inserted into the structure, it probably occupies the eightfold, cube-like coordination sphere for reasons of space, replacing two of the monovalent charged neighboring alkali metal cations. The black line in e) shows the measured luminescence spectrum of a CRNLLSO:Eu^{2+} single crystal. The dashed line represents the sum fit of the calculated blue and green luminescence peaks (λ_{exc} = 408 nm).

this point, it also becomes clear that the filling of CH1 or the Cs^+ content cannot be particularly relevant for luminescence. All such UCr_4C_4-type compounds known in the literature show a uniform blue luminescence band at 471–485 nm, regardless of whether the heavy-alkali-metal channel CH1 contains Cs^+, Rb^+, K^+, or Na^+. In these cases, much stronger shifts in the emission band would be expected for positioning of the emission center in CH1. The common feature of the above-mentioned compounds is that they all have light-alkali-metal channels CH2 that contain only Na^+.

A discontinuous change in the luminescence behavior only occurs in this compound class when lithium is located in CH2 (solely or in combination with Na^+). Detecting this requires single-crystal data, since the presence of Li^+ (in combination with Na^+) in the CH2 channel cannot be confirmed by PXRD data. This is why we propose that Eu^{2+} in an Li^+ domain generates the green emission peak. The latest publication by Dutzler et al. comes to a corresponding finding for $RbKLi_2[Li_3SiO_4]_4$:Eu^{2+} (RKLSO:Eu^{2+}).[16] In this compound, there are only Li^+ cations on the square-planar position in CH2 and the green luminescence is associated with a refinement of Eu^{2+} in the cube-like eightfold-coordinated position. Another indication of the correlation between green luminescence and Li^+ channels is also provided by additional single-crystal refinements from other approaches with varying refined Li^+ content. There is a discernable trend that $Cs_{4-x-y-z}Rb_xNa_yLi_z[Li_3SiO_4]_4$:$Eu^{2+}$ with a higher Li^+ content has a more intense green peak. Figure 3 shows the clear correlation between the position of the substances in the CIE diagram and the Li^+ content, in such a way that the color point shifts from cyan-blue to the green color range with increasing Li^+ content.

To recheck the general assumption that the activator ion migrates into CH2, as already been shown for RKLSO:Eu^{2+},[16] a

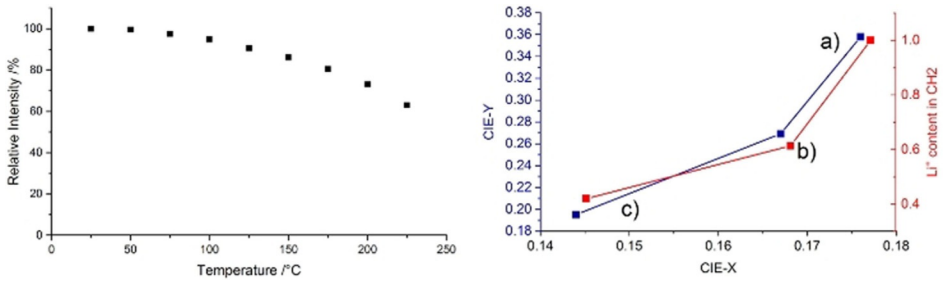

Figure 3. Left: Representation of the thermal quenching behavior of CRNLLSO as the relative integral photoluminescence intensity measured in steps of 25 °C from room temperature (25 °C) to 225 °C. Right: CIE plot of three refined single crystals from the CRNLLSO series with decreasing lithium content: a) $Cs_{0.451}Rb_{0.867}Na_{1.682}Li_1(Li_3SiO_4)_4$:$Eu^{2+}$, b) $Cs_{0.382}Rb_{0.706}Na_{2.298}Li_{0.614}(Li_3SiO_4)_4$:$Eu^{2+}$, and c) $Cs_{0.274}Rb_{0.792}Na_{2.514}Li_{0.42}(Li_3SiO_4)_4$:$Eu^{2+}$.

second refinement on the single-crystal was carried out, this time involving Eu^{2+}. A successful refinement was achieved with a mixed occupation of Eu^{2+} on the Na^+ site in CH2 towards the new sum formula $Cs_{0.445}Rb_{0.870}Na_{1.628}Eu_{0.06}Li_1[Li_3SiO_4]_4$. With final values of $R1 = 3.6\,\%$ and $wR2 = 10.0$, this is a slightly better result than without Eu^{2+} and, considering an effective initial Eu^{2+} weighting of 1 mol%, it is also plausible concerning the refined Eu^{2+} content.

Different emission colors therefore seem to be related to different vierer-ring channel types. The results argue for the eight-fold, cube-like coordination sphere in CH2 as a possible doping site, but exact determination of the Eu^{2+} centers is still infeasible with current methods.

Remarks on the syntheses

Considering the obtained sum formula, the non-integer stoichiometric ratios of the alkali metal ions are noticeable. In fact, the weighed sample was normally based on integer alkali metal ratios, such as $Cs_{4-x-y-z}Rb_xNa_yLi_z[Li_3SiO_4]_4:Eu^{2+}$ with a Cs:Rb:Na:Li:Si:O ratio of 2:1:1:13:4:16 for the example of the batch from which the refined single-crystals originated. Additional syntheses were done in an attempt to control the Na^+/Li^+ ratio in order to investigate the effects on luminescence. However, in terms of synthesis we had to face a few so far unsolvable challenges. First, it does not seem possible to target the stoichiometric ratios of the channel-filling alkali metal ions through the chosen synthesis method. An excess of cesium does not contribute to any further increase of the cesium content in the product, but it appears that excess Cs_2CO_3 acts as a flux and leads to the formation of some kind of pseudo-melt, which contributes to better crystallization. A sum formula in integer numbers, for example, $CsRbNaLi[Li_3SiO_4]_4$, is not feasible because of the space required by Cs^+ and Rb^+. Even when an excess of Cs^+ is applied, the Cs^+:Rb^+:Na^+ ratio in CH1 settles more or less by itself, and a higher Cs^+ content as in the described single crystal was never achieved. A similar situation can be found for CH2: Even with a deficiency of Na^+ and an excess of Li^+ or vice versa, the stoichiometry could not be adjusted in a targeted manner towards integer-number compositions. Especially at high Li^+ content, the crystallinity decreases sharply and it is more difficult to isolate single-crystals. At the same time, within the same batch, large fluctuations and inhomogeneities are observed in the composition of the single crystals. Actually, it seems that the initial weight of the starting materials has little impact on the final composition of the refined single-crystals, which is almost not at all controllable or influenced by targeted weighting or excess reagents.

To recheck the composition, energy-dispersive X-ray (EDX) spectroscopic measurements were conducted on powder particles of the product. All used elements could be detected, but the investigated individual crystallites had varying compositions. One reason for the deviation could be crystallization from a pseudo-melt with differing compositions of melt and crystallizing species. Nevertheless, EDX gives an indication of whether and to what extent the starting materials have reacted or whether, for example, complete evaporation of certain components has occurred, which seems not to be the case. Thus, an accurate phase analysis is difficult, but one can rely on the results of the single-crystal structure refinement owing to the high quality factors.

The inhomogeneity of the product is also reflected in the luminescence spectra. In Figure 4, the emission and excitation spectra for the green and blue maxima of the powder sample are depicted. Compared with the emission spectrum of the refined single crystal in Figure 2e, the intensity ratio of the green peak to the blue peak is much larger. This does not seem surprising, since reabsorption of the emitted blue radiation by the other emission center occurs in the powder, as can be seen from the overlap of the excitation spectra in Figure 4.

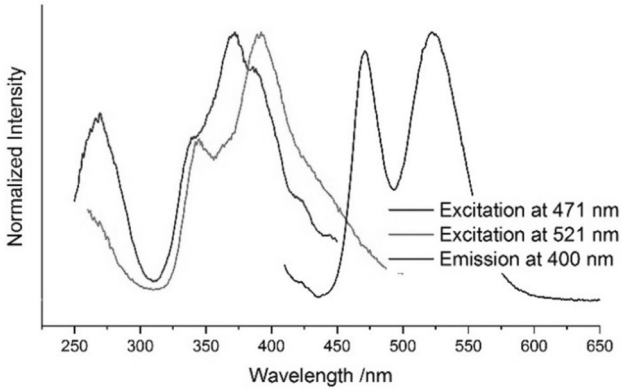

Figure 4. Excitation spectra (powder measurement) for the blue ($\lambda_{em} \approx 471$ nm) and green ($\lambda_{em} \approx 521$ nm) emission peaks in the corresponding colors. The black line shows the luminescence spectrum recorded at an excitation wavelength of 400 nm.

In addition, however, the position of the green luminescence maximum in the powder differs slightly from that of the single crystal. The peak maximum of the green-emitting powder sample was calculated to be 524.1 nm, and that of the single-crystal was calculated to 530.5 nm. The lower value for the powder sample cannot be due to reabsorption effects, as these would lead to a shift of the maximum to higher wavelengths. Given the suspected relationship between the position of the luminescence bands and the Li^+/Na^+ ratio, the effect can probably be explained by inhomogeneous composition in the powder.

Initial measurements of the quantum efficiency of laboratory samples were conducted. So far, without any optimization, values of about 40% have been achieved.

Conclusion

We were able to synthesize a new representative in the class of alkali metal lithosilicates, namely $Cs_{4-x-y-z}Rb_xNa_yLi_z[Li_3SiO_4]_4$, which exhibits luminescence properties when doped with the activator ion Eu^{2+}. It is hence added to a promising series of Eu^{2+}-doped alkali metal lithosilicates, which are claimed for their application as phosphor materials in a patent.[23] As the first member of this substance class, CRNLLSO has both Na^+

and Li^+ cations in its light-alkali-metal channels and shows unique double-band luminescence. It thus seems to combine the luminescence properties of $RbKLi_2[Li_3SiO_4]_4:Eu^{2+}$ and, for example, $RbNa_3[Li_3SiO_4]_4:Eu^{2+}$, which emit green and blue light, respectively. Investigations of the Na^+ and Li^+ sites in detail are only accessible by single-crystal measurements and lead to the assumption of domain formation regarding the light-alkali-metal vierer-ring channels. Thus, blue luminescence occurs when Eu^{2+} is incorporated into an Na^+ domain and green luminescence when it enters an Li^+ domain. Exact determination of the emission centers is not possible, but a correlation between the green-to-blue ratio and the Li^+:Na^+ ratio in the light-alkali-metal channel can be seen. This could mean that targeted control of the luminescence behavior by means of the blue/green ratio would be possible by variation of the composition. However, the challenge of controlling the exact composition and achieving homogeneity would still have to be mastered. Nonetheless, this interesting new alkali metal lithosilicate provides new insights into the luminescent properties of this compound class.

Experimental Section

Synthesis

$Cs_{4-x-y-z}Rb_xNa_yLi_z[Li_3SiO_4]_4:Eu^{2+}$ was synthesized by a conventional solid-state reaction in a tube furnace. The starting materials Cs_2CO_3 (107.1 mg, ChemPur, 99.99%), Rb_2CO_3 (38.0 mg, ChemPur, 99.9%), Na_2CO_3 (17.4 mg, ChemPur, 99.9%), Li_2CO_3 (157.9 mg, Fluka, 99.5%), SiO_2 (79.0 mg, Fluka, >99.9%), and Eu_2O_3 (0.6 mg, 1 mol%, Smart Elements, 99.9%) were weighed in inert gas atmosphere to prevent falsification of the masses due to hydration of the moisture-sensitive starting materials (argon atmosphere, UniLab Plus Glove Box Workstation, MBraun, Garching, Germany). Then, the compounds were ground in a planetary mill (Pulverisette 7, Fritsch, Idar-Oberstein, Germany) and transferred to open nickel crucibles. The mixture was fired with a heating rate of 3 °C min^{-1} at 750 °C for 4 h in a constant flow of forming gas (H10, Messer Austria GmbH) to induce the reduction from Eu^{3+} to Eu^{2+} and then cooled with a cooling rate of 1.5 °C min^{-1}. The obtained product can be stored over months under ambient conditions without detectable degeneration.

Single-crystal XRD

Single-crystals could be isolated from the crystalline powder by utilizing a polarization microscope. The crystallographic measurements were carried out at room temperature with a D8 Quest Kappa X-ray diffractometer (Bruker, Billerica, USA) with CuK_α radiation ($\lambda = 1.54178$ Å). The diffractometer was equipped with a microfocus X-ray tube (Incoatec, Geesthacht, Germany) combined with multilayer optics and a Photon II detector. A multiscan absorption correction of the intensity data was conducted using the software tools SAINT[24] and SADABS.[25] The structure was solved using Direct Methods provided by SHELXS[26] and refined with SHELXL[27] as implemented in the WinGX[28] suite.

CCDC 1953238 contains the supplementary crystallographic data for this paper. These data are provided free of charge by The Cambridge Crystallographic Data Centre.

EDX spectroscopy and electron microscopy

To check the composition of the product, EDX spectroscopy was conducted. A SUPRA 35 scanning electron microscope (CARL ZEISS, field emission) equipped with a Si/Li EDX detector (OXFORD INDUSTRIES, model 7426) was used.

Luminescence

Single-crystals of the new compound were mounted on glass fibers and their luminescence was measured by using a setup equipped with a UV-to-blue laser diode ($\lambda = 408$ nm, Thorlabs), a single-mode optical fiber S405XP (Thorlabs), and a QE 65000 spectrometer (Ocean Optics).

Luminescence data of the powder samples were recorded with a Fluoromax 4 spectrophotometer (Horiba). The emission spectrum was detected in the wavelength range between 410 and 750 nm (step size: 1 nm) with an excitation wavelength of 400 nm. Excitation spectra, monitored at the corresponding maximum intensity, were measured by the same method.

Acknowledgements

We would like to thank Christian Koch for the SEM-EDX measurements (OSRAM Opto Semiconductors).

Conflict of interest

The authors declare no conflict of interest.

Keywords: alkali metals · high-temperature chemistry · luminescence · silicates · solid-state structures

[1] a) P. Pust, P. J. Schmidt, W. Schnick, *Nat. Mater.* **2015**, *14*, 454 – 458; b) J. Cho, J. H. Park, J. K. Kim, E. F. Schubert, *Laser Photonics Rev.* **2017**, *11*, 1600147; c) M.-H. Fang, J. L. Leaño, Jr., R.-S. Liu, *ACS Energy Lett.* **2018**, *3*, 2573 – 2586; d) C. C. Lin, R.-S. Liu, *J. Phys. Chem. Lett.* **2011**, *2*, 1268 – 1277; e) S. Ye, F. Xiao, Y. Pan, Y. Ma, Q. Zhang, *Mater. Sci. Eng. R* **2010**, *71*, 1 – 34; f) Z. Xia, Q. Liu, *Prog. Mater. Sci.* **2016**, *84*, 59 – 117; g) Z. Xia, Z. Xu, M. Chen, Q. Liu, *Dalton Trans.* **2016**, *45*, 11214 – 11232.

[2] G. Blasse, A. Bril, *Appl. Phys. Lett.* **1967**, *11*, 53 – 55.

[3] a) N. Hirosaki, R.-J. Xie, K. Kimoto, T. Sekiguchi, Y. Yamamoto, T. Suehiro, M. Mitomo, *Appl. Phys. Lett.* **2005**, *86*, 211905; b) R.-J. Xie, N. Hirosaki, *Sci. Technol. Adv. Mater.* **2007**, *8*, 588.

[4] K. Uheda, N. Hirosaki, Y. Yamamoto, A. Naito, T. Nakajima, H. Yamamoto, *Electrochem. Solid-State Lett.* **2006**, *9*, H22 – H25.

[5] a) H. Höppe, H. Lutz, P. Morys, W. Schnick, A. Seilmeier, *J. Phys. Chem. Solids* **2000**, *61*, 2001 – 2006; b) R. Mueller-Mach, G. Mueller, M. R. Krames, H. A. Höppe, F. Stadler, W. Schnick, T. Juestel, P. Schmidt, *Phys. Status Solidi A* **2005**, *202*, 1727 – 1732; c) K. Uheda, N. Hirosaki, H. Yamamoto, *Phys. Status Solidi A* **2006**, *203*, 2712 – 2717; d) M. R. Krames, G. O. Mueller, R. B. Mueller-Mach, H.-H. Bechtel, P. J. Schmidt, *Wavelength Conversion for Producing White Light from a High Power Blue Light Emitting Diode (LED).* U.S. Patent Application No. 12/464,327, **2010**.

[6] J. K. Park, C. H. Kim, S. H. Park, H. D. Park, S. Y. Choi, *Appl. Phys. Lett.* **2004**, *84*, 1647 – 1649.

[7] J. K. Park, K. J. Choi, J. H. Yeon, S. J. Lee, C. H. Kim, *Appl. Phys. Lett.* **2006**, *88*, 043511.

[8] a) R. Werthmann, R. Hoppe, *Z. Anorg. Allg. Chem.* **1984**, *509*, 7 – 22; b) B. Nowitzki, R. Hoppe, *Rev. Chim. Miner.* **1986**, *23*, 217 – 230; c) K. Bernet, R. Hoppe, *Z. Anorg. Allg. Chem.* **1991**, *592*, 93 – 105; d) J. Hoffmann, R. Brandes, R. Hoppe, *Z. Anorg. Allg. Chem.* **1994**, *620*, 1495 – 1508.

[9] D. Dutzler, M. Seibald, D. Baumann, H. Huppertz, *Angew. Chem. Int. Ed.* **2018**, *57*, 13676 – 13680; *Angew. Chem.* **2018**, *130*, 13865 – 13869.

[10] M. Iwaki, S. Kumagai, S. Konishi, A. Koizumi, T. Hasegawa, K. Uematsu, A. Itadani, K. Toda, M. Sato, *J. Alloys Compd.* **2019**, *776*, 1016 – 1024.
[11] M. Zhao, H. Liao, M. S. Molokeev, Y. Zhou, Q. Zhang, Q. Liu, Z. Xia, *Light: Sci. Appl.* **2019**, *8*, 38.
[12] M. Zhao, H. Liao, L. Ning, Q. Zhang, Q. Liu, Z. Xia, *Adv. Mater.* **2018**, *30*, 1802489.
[13] H. Liao, M. Zhao, Y. Zhou, M. S. Molokeev, Q. Liu, Q. Zhang, Z. Xia, *Adv. Funct. Mater.* **2019**, *29*, 1901988.
[14] M. Zhao, Y. Zhou, M. S. Molokeev, Q. Zhang, Q. Liu, Z. Xia, *Adv. Opt. Mater.* **2019**, *7*, 1801631.
[15] H. Liao, M. Zhao, M. S. Molokeev, Q. Liu, Z. Xia, *Angew. Chem. Int. Ed.* **2018**, *57*, 11728 – 11731; *Angew. Chem.* **2018**, *130*, 11902 – 11905.
[16] D. Dutzler, M. Seibald, D. Baumann, F. Philipp, S. Peschke, H. Huppertz, *Z. Naturforsch. B* **2019**, *74*, 535 – 546.
[17] F. Liebau in *Structural Chemistry of Silicates*, Springer, Berlin, **1985**.
[18] P. Pust, V. Weiler, C. Hecht, A. Tücks, A. S. Wochnik, A.-K. Henß, D. Wiechert, C. Scheu, P. J. Schmidt, W. Schnick, *Nat. Mater.* **2014**, *13*, 891.
[19] G. J. Hoerder, M. Seibald, D. Baumann, T. Schröder, S. Peschke, P. C. Schmid, T. Tyborski, P. Pust, I. Stoll, M. Bergler, *Nat. Commun.* **2019**, *10*, 1824.
[20] J. Qiao, L. Ning, M. Molokeev, Y.-C. Chuang, Q. Zhang, K. Poeppelmeier, Z. Xia, *Angew. Chem. Int. Ed.* **2019**, *58*, 11521 – 11526; *Angew. Chem.* **2019**, *131*, 11645 – 11650.
[21] N. Wiberg, E. Wiberg, A. Holleman, *Lehrbuch der anorganischen Chemie*, de Gruyter, Berlin **2007**.
[22] M. Chen, Z. Xia, M. S. Molokeev, C. C. Lin, C. Su, Y.-C. Chuang, Q. Liu, *Chem. Mater.* **2017**, *29*, 7563 – 7570.
[23] M. Seibald, D. Baumann, T. Fiedler, S. Lange, H. Huppertz, D. Dutzler, T. Schröder, D. Bichler, G. Plundrich, S. Peschke, G. Hoerder, G. Achrainer, K. Wurst, WO/2018/029304, **2018**.
[24] SAINT, v8.34a, Bruker AXS Inc., Madison, WI, USA, **2014**.
[25] L. Krause, R. Herbst-Irmer, G. M. Sheldrick, D. Stalke, *J. Appl. Crystallogr.* **2015**, *48*, 3 – 10.
[26] G. M. Sheldrick, *Acta Crystallogr. Sect. A* **2008**, *64*, 112 – 122.
[27] G. M. Sheldrick, *Acta Crystallogr. Sect. C* **2015**, *71*, 3 – 8.
[28] STOE Win XPOW, Version 2.23, S. C. GmbH, Darmstadt, **2005**.

Manuscript received: October 2, 2019
Revised manuscript received: November 8, 2019
Accepted manuscript online: November 11, 2019
Version of record online: January 21, 2020

